

LA-UR-16-21748

Approved for public release; distribution is unlimited.

Title: (U) Design Considerations for Obtaining Deep Release in Reacted Epon 828

Author(s): Fredenburg, David A.
Lang, John Michael Jr.
Dattelbaum, Dana Mcgraw
Bennett, Langdon Stanford

Intended for: Report

Issued: 2016-03-16

Disclaimer:

Los Alamos National Laboratory, an affirmative action/equal opportunity employer, is operated by the Los Alamos National Security, LLC for the National Nuclear Security Administration of the U.S. Department of Energy under contract DE-AC52-06NA25396. By approving this article, the publisher recognizes that the U.S. Government retains nonexclusive, royalty-free license to publish or reproduce the published form of this contribution, or to allow others to do so, for U.S. Government purposes. Los Alamos National Laboratory requests that the publisher identify this article as work performed under the auspices of the U.S. Department of Energy. Los Alamos National Laboratory strongly supports academic freedom and a researcher's right to publish; as an institution, however, the Laboratory does not endorse the viewpoint of a publication or guarantee its technical correctness.

(U) Design Considerations for Obtaining Deep Release in Reacted Epon 828

D.A. Fredenburg,* J.M. Lang, D.M. Dattelbaum, and L.S. Bennett
Los Alamos National Laboratory, Los Alamos, NM 87545
(Dated: March 14, 2016)

This document summarizes results from one-dimensional calculations performed to investigate the release behavior of reacted Epon 828. Two design goals were set, (1) the product phase had to be achieved upon the initial shock loading, and (2) a deep release state could be achieved. Both transmission and front surface impact geometry were investigated. The two design criteria were met with the front surface impact design employing a modified projectile.

I. INTRODUCTION

A series of experiments are planned to investigate the release behavior of Epon 828 following transition of the material to its product phase upon shock loading. Specifically, these experiments seek to determine if the release path lies above or below the reactant phase Hugoniot. The current reactant-product equation of state (EOS) treatment for Epon 828 is shown in Fig. 1.[1, 2] In this configuration the material originates in the reactant phase on EOS 7603, and remains in the reactant phase for shock pressures up to approximately $P = 24$ GPa, or a specific volume of $V = 0.509 \text{ cm}^3/\text{g}$. When shock pressures are increased, the material response deviates from that predicted by the reactant phase and is thought to transition to a product. The product response is captured with EOS 97605, and is calibrated primarily by existing shock data at pressures above the transition.

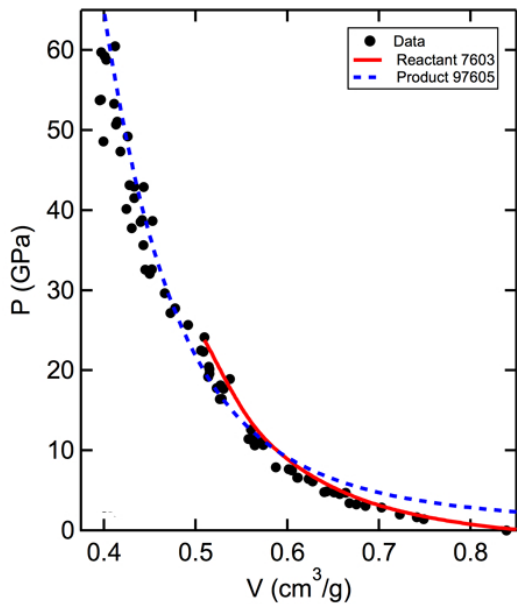


FIG. 1. Experimental shock Hugoniot data for Epon 828 shown with reactant (7603) and product (97605) EOS.

Inspection of Fig. 1 reveals that the equilibrium EOS for the product phase extends well below the transition pressure, where in the 10-20 GPa range the product curve falls below and to the left of the reactants. As pressures decrease below 10 GPa, the product phase crosses the reactant Hugonot, now lying above and to the right of the reactant EOS. With very little known about the deep release response of reacted polymer systems, the low-pressure product behavior observed in Fig. 1 is largely a consequence of modeling choices in the theoretical development of the product phase EOS. To gain further insight into the release behavior of Epon 828, a series of experiments are designed for the Ancho Canyon two-stage explosively driven planar impact gun. There are two design goals for these experiments, (1) achieving the product phase of Epon 828 upon the initial shock, and (2) achieving a deep release in the Epon where pressures upon release are below that of the initial transition, below ~ 24 GPa. This document describes results from calculations representing several experimental design iterations aimed at meeting the above two design goals.

II. EXPERIMENTAL

As the calculations performed in the later part of this document are aimed at helping to inform the design of experiments, it is first necessary to discuss the scope and limitations of the platform on which these experiments are to be performed. The Ancho Canyon two-stage gun at LANL provides the drive necessary to reach the product phase of Epon on initial shock loading. For this gun, the barrel of the launch tube is 28 mm, and its impact velocity (U_D) range is approximately 2.5 - 6.5 km/s. For a deep release experiment the ideal loading scenario is such that a high impedance material initially shocks the Epon into the high pressure phase, after which a release wave (isentrope) travels through the Epon and unloads the material to a state well below the initial transition pressure from reactant to product. In achieving these states in the Epon, one must simultaneously be able to measure the loading and unloading states via a time-resolved diagnostic.

The optimal diagnostic for this type of experiment would be some form of embedded diagnostic that measures the pressure state of Epon directly, while simulta-

* dafreden@lanl.gov
Tel: (505)-667-5300
LA-UR-16-XXXXX

neously not interfering with the dynamics of wave propagation in the target. While embedded magnetic gauges have been used previously at LANL to measure the shock and unloading characteristics of explosives and other materials,[3–5] these diagnostics are not currently available for use on the Ancho Canyon two-stage gun. The primary diagnostic at the Ancho Canyon gun facility is optical velocimetry, where both VISAR[6] and PDV[7] are regularly fielded. As such, any proposed design must utilize optical windows for measuring velocimetry traces at the Epon/window interface.

Another experimentally-driven design consideration is that of the structural integrity of the projectile. Initially at rest in the interstage region between the first and second stages of the gun, the projectile is accelerated to velocities of several kilometers per second over the course of a few milliseconds. These intense accelerations make design of the projectile an integral consideration. Historical experience has limited the projectile to a standard metal impactor embedded within a molded Lexan projectile. As such, initial design considerations were limited to this configuration. However, later design iterations were forced to explore alternate projectile designs, as the conventional projectile design was not able to achieve the two design goals. The first series of calculations were in the transmission geometry, and are discussed in the following section. The second series of calculations were in the front surface impact configuration, the results of which are discussed last.

III. TRANSMISSION GEOMETRY

Building on previous experiments on polymeric systems, the initial design proposed was in the transmission geometry, where the target consists of an Epon sample sandwiched between a high impedance impactor and a low impedance window, impacted by a high impedance material in the projectile. For a single-slug experiment, the 28 mm bore diameter can accommodate relatively thick Epon samples while still keeping the sample height to diameter (H:D) ratio relatively low. Therefore, in designing these experiments a wide range of sample thicknesses can be examined to ensure the appropriate physics of the release behavior are captured within the time scale of the experiment. To optimize the transmission geometry, a series of one-dimensional calculations were performed over a range of impact scenarios with the LANL hydrocode FLAG.[9] The following sub-sections give the results of the calculations performed in the transmission geometry in greater detail.

A. Lexan-Backed Calculations

The first series of calculations were performed in the standard transmission geometry with the standard projectile, flyer plate, impactor, and window materials. A

schematic of the one-dimensional geometry is given in Fig. 2. Standard dimensions for this, and the remaining transmission geometry calculations, were that the Lexan sabot was 16 mm in length, the Cu baseplate was 1.0 mm in length, and the LiF window was 9.0 mm in length. Thicknesses for the Cu impactor and the Epon 828 were varied to determine if the appropriate physical response at the optical velocimetry interface between the Epon 828 and the LiF window could be measured. Recall the two design goals: (1) initial shock into the product phase, and (2) deep release in the Epon. Furthermore, is also desired that the temporal duration of the release is maximized, such that the lowest possible release state in the Epon 828 sample can be obtained.

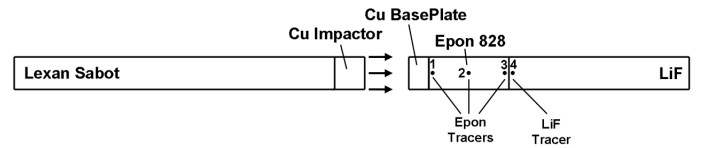


FIG. 2. Geometry for one-dimensional calculations with Lexan backer.

The first calculations were optimized at an impact velocity of $U_D = 5.0$ km/s, which consisted of a 1.5 mm Cu impactor and a 4.0 mm Epon 828 sample, in addition to the standard thicknesses given previously. This impact condition was chosen to result in an initial state on the product EOS only slightly above the transition from reactant to product. A series of material velocity profiles from tracer particles in the Epon 828 and the LiF (see Fig. 2 for location) are plotted in Fig. 3(a). For the tracer nearest the baseplate/sample interface, T1, the material velocity rises sharply to its peak state, where it stays for $\sim 0.4 \mu\text{s}$ before the release wave from the Lexan/Cu interface causes the material velocity to decrease. The tracer in the middle of the Epon 828, T2, experiences a similar rise, plateau, and initial release; however approximately $0.1 \mu\text{s}$ after the start of the release, a sharp drop in material velocity is observed. This drop in material velocity corresponds to the initial shock being reflected at the sample/window interface. Because the LiF window is higher impedance than the Epon 828, the reflected wave is a shock, causing an increase in pressure, see Fig. 3(b) and a corresponding decrease in material velocity. The Epon tracer nearest the Epon/LiF interface, T3, only experiences the peak material velocity state for a very short time before the reflected shock from the LiF results in a lower material velocity state.

The material velocity trace given by T4 in the LiF is representative of what is actually measured by optical velocimetry in the experiment. In this trace, the material velocity is observed to be shocked up to its initial peak state of around $u_P = 3.0$ km/s, where the peak state is maintained for $\sim 0.1 \mu\text{s}$ before release occurs. The release in the LiF is calculated to reduce to approximately 1.5 km/s before additional wave interactions cause a subsequent shock at the interface.

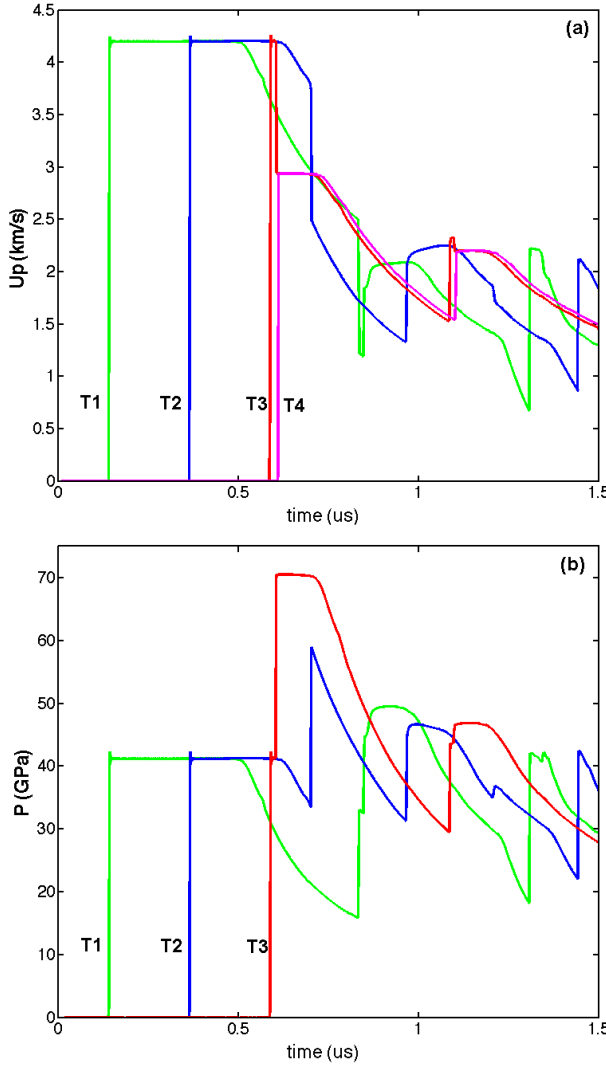


FIG. 3. Results for u_p and P from tracer particles in one-dimensional experiments for $U_D = 5.0$ km/s.

Results from the calculations examining the material response in terms of pressure are shown in Fig. 3(b). Here the initial shock is observed to result in a shock pressure of 40 GPa. Inspection of the P - V Hugoniot response given in Fig. 1 reveals that at 40 GPa the material exists at the lower end of the transitioned product Hugoniot, thereby meeting design criteria (1). The second design criteria was to produce and measure a deep release state in the product phase of Epon 828. Examination of the pressure recorded at the tracer in the Epon nearest to the LiF window, T3, shows that the initial pressure of 40 GPa in the Epon is quickly increased to nearly 70 GPa as a result of the re-shock of the Epon from the LiF. From this elevated pressure state, the pressure is observed to release to nearly 30 GPa before additional wave interactions cause a subsequent re-shock in the material. Therefore, the present transmission geometry is unable to access a deep release state; rather, this ex-

periment would only provide information on the release trajectory of Epon from 70 to 30 GPa.

While the current geometry was able to meet the first design goal of achieving the product phase in Epon upon initial shock loading, it was not able to achieve a deep release state in the Epon. The limiting factor on achieving the deep release state may be rooted in two causes. The first is a result of the Lexan backer for the Cu impactor. Lexan is a relatively modest low impedance backer, and a deeper release state may be achieved if a lower impedance backer could be used in these experiments, for example, TPX. The second reason a deep release state may not be able to be achieved is due to the relatively high impedance of the LiF window, resulting in a re-shocked state in the Epon that is much higher than the initial shock pressure. The next set of calculations investigates the use of a lower impedance backer material for the impactor.

B. TPX-Backed Calculations

To examine the influence of the backer impedance on the final release state in the Epon, a series of calculations were performed where the Lexan backer in the previous calculations was replaced with a lower impedance TPX plastic.[8] A schematic of the one dimensional setup is shown in Fig. 4. In this configuration, the left traveling shock in the Cu impactor now interacts with TPX instead of Lexan, and should release to a lower overall pressure state. However, inspection of the wave profiles for the Lexan backed calculations given in Fig. 3 reveals that the re-shock from the LiF may overdrive the Epon such that a deep release in the Epon may not be reached by simply replacing the backer with TPX.

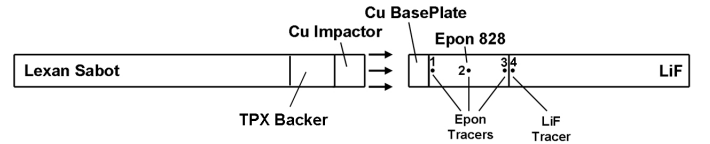


FIG. 4. Geometry for one-dimensional calculations with TPX backer.

To investigate the extent by which replacing the backer material from Lexan to TPX has on the final release state achieved in Epon, the previous calculations at an impact velocity of $U_D = 5.0$ km/s were repeated with the insertion of a 5 mm TPX backer between the Cu impactor and the Lexan sabot. For these calculations a 1.5 mm Cu impactor and 4.0 mm Epon 828 sample were used, with other nominal dimensions remaining the same. It should be noted that such a projectile, where the impactor is supported by a low-impedance backer has not been experimentally vetted.

Inspection of material velocity and pressure profiles from the tracer particles for the TPX-backed calculations were qualitatively similar to those where the impactor

was backed by Lexan. To investigate whether or not the TPX backer was able to lower the final release state in the Epon prior to the late time wave interactions that cause a re-shock in the Epon, the pressure traces from both the Lexan- and TPX-backed calculations are examined together. Results from tracer T3 in the Epon at a distance of $100\ \mu\text{m}$ from the Epon/LiF interface for both the Lexan- and TPX-backed calculations at $U_D = 5.0\ \text{km/s}$ are shown in Fig. 5.

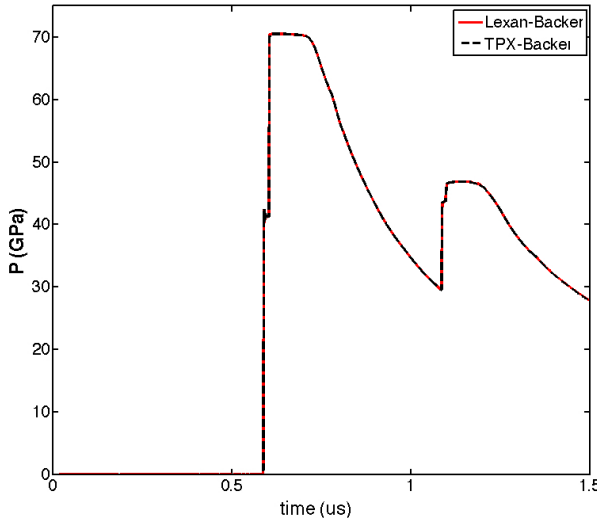


FIG. 5. Comparison of pressure traces in Epon 828 at T3 for Lexan and TPX backed Cu at $U_D = 5.0\ \text{km/s}$.

The initial shock pressure in the Epon is approximately 40 GPa for both geometries, which is increased to nearly 70 GPa upon re-shock of the Epon from the LiF window. Passage of the release wave resulting from the backer material (Lexan or TPX) causes a release from the high-pressure state; however, subsequent wave interactions only allow for the pressure to reach approximately 30 GPa in the Epon prior to re-shock. Therefore, while the TPX backer may decrease the final pressure state achievable, wave interactions resulting from the Epon/LiF interface preclude this deep release state from being achieved. As such, introducing a TPX backer does not allow for a deeper release state to be achieved in the Epon sample in the transmission geometry. Therefore, in the transmission geometry a deep release state in the Epon that extends into the region of phase space where the reactant phase EOS is initially active ($0 \leq P \leq 24\ \text{GPa}$) is not likely to be achieved without modification of the window to a lower impedance material or with alternate target geometries.

C. TPX Window Calculations

Here, alternate window materials were investigated to see if a suitable window could be found that would allow for a deep release state in the Epon to be achieved.

Window materials such as sapphire and quartz were deemed inappropriate due to their relatively high shock impedance. Polymer windows like PMMA have much more attractive shock impedances; however, PMMA turns optically reflective to common optical velocimetry techniques at pressures in excess of $\sim 25\ \text{GPa}$. An alternate low density polymer that has been used as a window material in shock Hugoniot experiments is TPX[8], which has also been measured experimentally to become optically reflective above some threshold pressure.[10] However, the actual threshold for this transition has not been determined. As such, TPX is examined further as a potential window material for obtaining deep release states in TPX in the transmission geometry.

To investigate the range of pressures accessed in a TPX window in the transmission geometry, and the corresponding release state achieved in Epon, a series of one dimensional calculations were performed with the geometry shown in Fig. 6. As it is likely that the transition to optical reflectiveness occurs in a pressure range near that of PMMA, calculations were only performed at the lower end of impact velocities necessary to reach the product phase of Epon 828 upon initial shock loading. All dimensions for the Lexan, TPX backer, Cu Impactor, Cu baseplate, Epon sample, and window (now TPX) are similar to the previous TPX-backed calculations. The primary variable in this set of calculations was the impact velocity, which was varied from $U_D = 4.5 - 5.0\ \text{km/s}$ to determine if a suitable combination of pressure in the Epon and TPX could be achieved that might allow for a deep release state in the Epon to be measured using optical velocimetry at the Epon/TPX window interface.

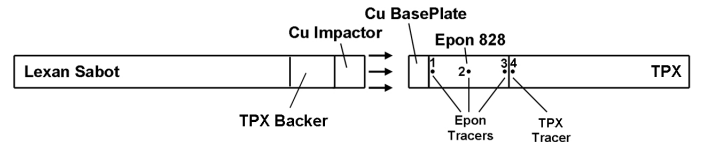


FIG. 6. Geometry for one-dimensional calculations with TPX backer and TPX window.

Results from tracer particles located near the impact face of the Epon 828 sample (T1) and TPX window (T4) for this series of calculations are shown in Fig. 7. In Fig. 7(a) varying the impact velocity from $U_D = 4.5 - 5.0\ \text{km/s}$ results in pressures in the Epon ranging between 34.8 - 41.2 GPa. Inspection of the reactant and product Hugoniots with the corresponding experimental data for Epon 828 given in Fig. 1 reveals that the transition from reactant to product begins at around 24 GPa and is fully transformed to the product phase near 30 GPa. Therefore, in all instances of impact velocity investigated, the Epon should be fully transformed to the product phase.

Examination of the pressure traces from the TPX window in Fig. 7(b) shows that the initial pressures experienced by the TPX range between 29.1 - 34.5 GPa. Therefore, at the lowest impact velocity investigated, $U_D = 4.5$

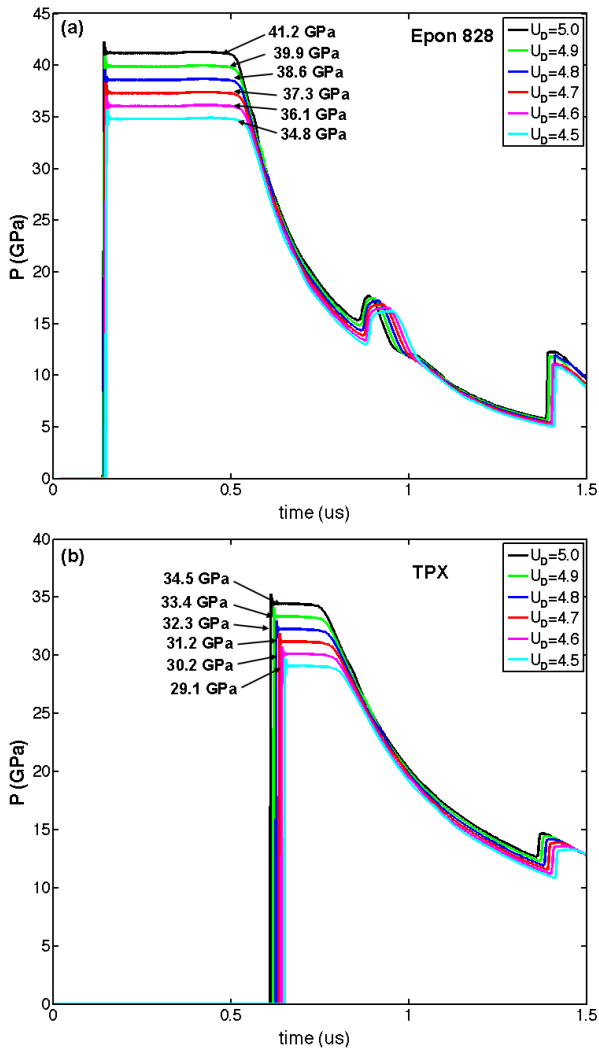


FIG. 7. Pressure traces illustrating the (a) pressure in the Epon 828 at T1 and (b) pressure in the TPX window at T4 for various impact velocities.

km/s, it may be possible to both fully react the Epon 828 and to measure the release state using a TPX window if the transition to optical reflectiveness in TPX is above 29 GPa. The final release state achieved in the Epon is also shown in Fig. 7(a), which indicates that pressures as low as \sim 15 GPa can be achieved. Inspection of the EOS plot in Fig. 1 shows that 15 GPa is well within the range of pressures where the reactant EOS is initially active, such that the present combination of impact velocity, TPX backer, and TPX window can achieve both the initial transition to the product phase and the deep release state in Epon. The only question remains is whether or not TPX transitions to optically reflective at pressures in excess of 29 GPa.

Due to the uncertainty in the optical reflectiveness of TPX, a single calculation was performed where the TPX window was replaced by PMMA, whose transition from optically transmissible to optically reflective is bet-

ter characterized. In these calculations PMMA was assigned the Lexan SESAME EOS, and all other geometries and tracer locations are similar to those for the $U_D = 4.5$ km/s calculations for the TPX window. The impact velocity was set to $U_D = 4.5$ km/s for the PMMA window calculations for direct comparison with those performed on the TPX window. Results of the pressure from tracers T4 in the windows are shown for both the PMMA and TPX windows in Fig. 8.

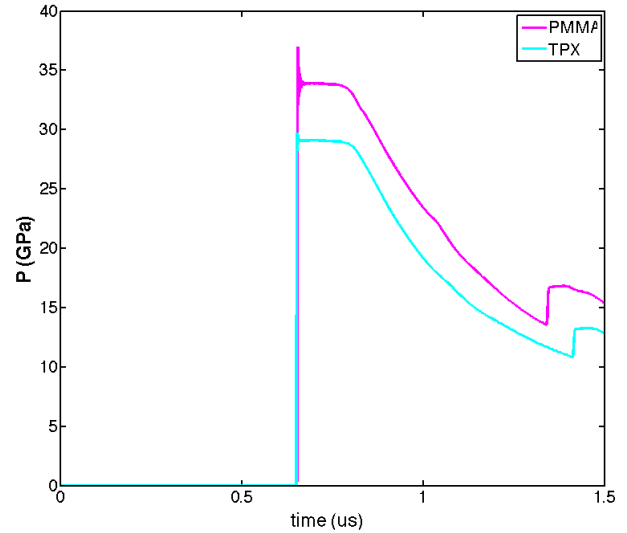


FIG. 8. Pressure traces illustrating differences in pressure at the Epon/window interface for the PMMA and TPX windows.

Inspection of Fig. 8 reveals that the pressure in the PMMA window is 33.9 GPa, while that in the TPX window is 29.1 GPa. It should be noted that PMMA (as represented in the calculation as Lexan) is a near perfect impedance match with Epon 828. Thus the pressure wave traveling through the Epon at $P = 34.5$ GPa is reduced only slightly upon transmitting into the PMMA window to a value of 33.9 GPa. For the lower impedance TPX window the pressure in the Epon is reduced further to 29.1 GPa. Therefore, while the final pressure state achieved with a PMMA window allows for the deep release state in the Epon to be realized, the initial pressure in the PMMA exceeds that which is required to reach optical reflectivity such that optical velocimetry can not be used to directly measure the release path.

Substitution of the LiF window with a TPX window has been identified as a possible means of satisfying both of the design criteria set forth in the present investigation. However, the range of pressures over which TPX can be used as an optically transmissive window for velocimetry measurements is not presently known. Therefore, it is likely that if TPX can be used at a window, it may only be used so to access pressures in the Epon 828 near those required to transition to the product phase, as demonstrated in the present calculations. Given the underlying uncertainty surrounding the pressure at which

TPX becomes optically reflective, a second design geometry whereby the Epon is impacted directly into a high impedance window was investigated.

IV. FRONT SURFACE IMPACT EXPERIMENTS

The second design geometry investigated was that corresponding to front surface impact (FSI) experiments. In this configuration, the sample (Epon) is impacted directly on the window, and optical velocimetry measures the velocity history at the sample/window interface. To increase the chances by which an appropriate deep release state in Epon is achieved, the Epon in these calculations was backed by a layer of low density epoxy-infiltrated glass micro balloons. The glass micro balloon (GMB) mixture was modeled computationally as fused quartz (SESAME EOS 7387) with an initial porous density of 0.56 g/cm^3 , where a ramp model with slope $a = 3.406 \times 10^{-6} \text{ Mbar/cm}^3$ was used to transition the material from its initially porous state to a state on the EOS. A schematic of the one-dimensional geometry associated with the FSI experiments is given in Fig. 9, where linear dimensions of the sabot, GMB, Epon, and LiF materials were 16, 4.0, 3.0, and 19 mm, respectively.

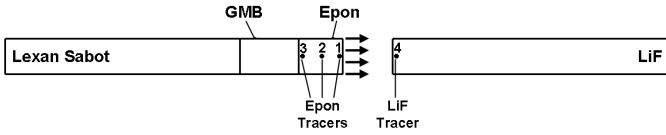


FIG. 9. Geometry for one-dimensional FSI calculations with GMB backer and LiF window.

In these calculations, it was desired to determine whether or not the Epon could be shocked to a state on the product Hugoniot upon initial impact with a LiF window, and then subsequently deep released to a low-pressure state. To examine this, a series of calculations were performed with the geometry shown in Fig. 9 at different impact velocities. Results showing the pressure traces in the Epon from tracer T1 at the Epon/LiF interface at impact velocities $U_D = 5.00, 5.25, 5.50$, and 5.75 km/s are given in Fig. 10. Results from the lowest impact velocity indicated that an initial pressure of $P = 29.8 \text{ GPa}$ is reached in the Epon, while at the top end of impact velocities the initial pressure is $P = 36.8 \text{ GPa}$. Examination of the EOS behavior in Fig. 1 indicates that the Epon should be fully transformed to the product phase upon impact at all of the velocities investigated. Further, upon release the pressures in the Epon are reduced to between $12.4 - 16.0 \text{ GPa}$, well below the transition region near 24 GPa , thus satisfying both design criteria.

The calculated pressures shown in Fig. 10 suggest that the FSI configuration, where GMB-backed Epon is impacted directly on a LiF window, can achieve both trans-

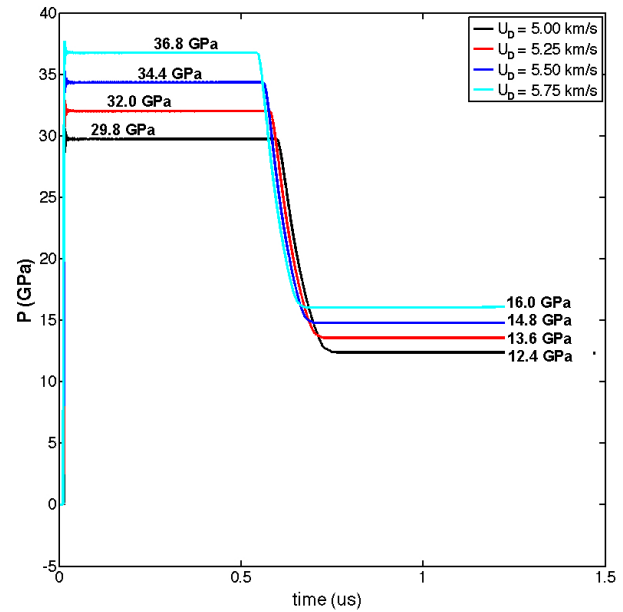


FIG. 10. Pressure traces in the Epon at the Epon/LiF interface (T1) for impact velocities of $U_D = 5.00, 5.25, 5.50$, and 5.75 km/s .

sition to the product phase upon initial impact, and a deep release state well below the initial transition pressure. As a result, the FSI geometry is proposed as the experimental design by which to investigate the deep release behavior of reacted Epon 828. Given that layered projectiles such as the one proposed by the current set of calculations have not yet been tested experimentally, it is recommended that structural integrity of the projectile be initially tested at the lower impact velocity of 5.00 km/s .

V. CONCLUSION

Calculations were performed in several different geometries to determine if it were possible to utilize optical velocimetry techniques to experimentally measure the shock response of Epon 828 that is transformed to the product phase upon the initial shock, and subsequently released to a low-pressure state. The initial transmission geometry consisting of the Epon sandwiched between a high impedance impactor and a window was unable to meet these design requirements. The design space was expanded to include a new projectile design for the Ancho Canyon two-stage gun that modified the projectile to include glass micro balloon (GMB)-backed Epon, such that a front surface impact (FSI) configuration could be tested. Calculated pressure traces from within the Epon demonstrated that the proposed FSI geometry could achieve both transition of the Epon to the product phase upon initial impact, and a deep release state following reflection of the shock from the GMB/Epon interface.

The FSI geometry shown in Fig. 9 is proposed as the experimental design by which to experimentally determine information about the release behavior of Epon 828 from the high-pressure product phase.

ACKNOWLEDGMENTS

This work was conducted at Los Alamos National Laboratory, an affirmative action/equal opportunity employer, which is operated by Los Alamos National Security, LLC, for the National Nuclear Security Administration of the U.S. Department of Energy under contract DE-AC52-06NA25396.

- [1] J.D. Coe, *SESAME Equations of State for "Epoxy"*, LANL Report, LA-UR-15-23248 (2015).
- [2] J.C. Boettger, *Sesame Equation of State for Epoxy*, LANL Report, LA-12755-MS (1994).
- [3] V.W. Manner, S.A. Sheffield, D.M. Dattelbaum, D.B. Stahl, in *Shock Compression of Condensed Matter - 2011* AIP Conf. Proc. 1426, pp. 201-204 (2012) doi: 10.1063/1.3686254.
- [4] L.L. Gibson, S.A. Sheffield, D.M. Dattelbaum, D.B. Stahl, in *Shock Compression of Condensed Matter - 2011* AIP Conf. Proc. 1426, pp. 323-326 (2012) doi: 10.1063/1.3686284.
- [5] D.M. Dattelbaum, S.A. Sheffield, in *Shock Compression of Condensed Matter - 2011* AIP Conf. Proc. 1426, pp. 627-632 (2012) doi: 10.1063/1.3686357.
- [6] L.M. Barker, R.E. Hollenbach, *J. Appl. Phys.* **43** (1972) 4669.
- [7] O.T. Strand, D.R. Goosman, C. Martinez, T.L. Whithworth, *Rev. Sci. Instrum.* **77** (2006) 083108.
- [8] D.A. Fredenburg, T.D. Aslam, L.S. Bennett, *(U) A Grüneisen Equation of State for TPX: Application in FLAG*, LANL Report, LA-UR-15-28533 (2015).
- [9] FLAG Code Manual: 3.6.Alpha.5, Maintained by: shavano-core@lanl.gov, June 18, 2015.
- [10] S. Root, T.R. Mattsson, K. Cochrane, R.W. Lemke, M.D. Knudsen, *Shock Compression Response of Poly(4-Methyl-1-Pentene) Plastic to 985 GPa*, unpublished (2015).